TNXB MUTATIONS IS A CAUSE OF VESICOURETERAL REFLUX (VUR)

*Rasheed A. Gbadegesin[1,2], Patrick D. Brophy[3], Adebowale Adeyemo[4], Gentzon Hall[5,2], Indra R. Gupta[6], David Hains[7], Bartlomeij Bartkowiak[1], C. Egla Rabinovich[8], Settara Chandrasekharappa[4], Alison Homstad[1,2], Katherine Westreich[1], Guanghong Wu[5,2], Yutao Liu[5,2], Danniele Holanda[9], Jason Clarke[3], Peter Lavin[5,2,10], Angelica Selim[11], Sara Miller[11], John S. Wiener[12], Sherry S. Ross[12], John Foreman[1], Charles Rotimi[4], Michelle P. Winn[5,2]

SUPPLEMENTARY MATERIALS

SUPPLEMENTARY METHODS

Scratch wound healing assay

Fibroblast cell line was established by culturing skin biopsy samples in modified DMEM. Cells were seeded on collagen-1 coated plates and allowed to grow to confluence prior to scratch wound creation. Scratch wounds were applied using 1000 µL pipet tip. Fibroblasts were treated with platelet derived growth factor (PDGF) (Cell Signaling, Inc.; Beverly, MA) at a concentration of 50 ng/ml or vehicle prior to being returned to 37^0C growth conditions for incubation for 15 hours. Fibroblast wound healing images at 0 and 15 hours were obtained using an EVOS® microscope and wound healing was quantified in 4 experiments as the % wound closure.

Immunoblotting and reagents

Following treatment, human epidermal fibroblast cultures were washed with PBS. Cells were harvested in RIPA buffer (Cell Signaling Technologies, Boston, MA, USA). Cell lysates were subjected to SDS-polyacrylamide gel electrophoresis. Protein immunoblotting was performed using rabbit polyclonal anti-FAK antibody or rabbit polyclonal anti-phospho-FAK (Tyr 397) antibody, or rabbit polyclonal TNXB antibody (Proteintech, Inc; Chicago, IL). Immunolabeled proteins were detected using a chemiluminescence detection system (Pierce Biotechnology, Rockford, IL, USA) on Kodax BioMax film (VWR Scientific).

Immunohistochemical and Immunofluorescence staining of the UVJ junction

Paraffin embedded human tissue samples were obtained from the pathology department at the University of Iowa under approval of Institutional Board Review protocol # 200901770. Normal controls were obtained from autopsy specimens and

compared to specimens isolated from individuals with radiographically demonstrated reflux who underwent surgical re-implantation. Block samples were sectioned via microtome into 5-7 micron sections and affixed to microscopy slides. Immunohistochemistry and Immunofluorescence was performed on slide sections that had undergone heating to 55^{o}C and allowed to cool to room temperature. Slides were cleared twice with xylene for 5 minutes. Slide samples were hydrated through a reducing ethanol bath series and rinsed with distilled water and PBS. Slides were then submerged in boiling citrate buffer (10 mM, Ph 6.0), allowed to cool for 1 minute, resubmerged and allowed to cool for 20 minutes to room temperature in antigen retrieval solution. A.) For Immunohistochemistry: Slides were rinsed with distilled water and endogenous peroxidase activity was blocked with 3% hydrogen peroxidase in PBS for 20 min. Slide sections were then rinsed with PBS and incubated with 5% normal goat serum/5% Bovine Serum Albumin for 1 hr at room temp. Avidin-Biotin activity was blocked using a kit: (Invitrogen, Avidin/Biotin Blocking Kit, Cat#: 00-4303) as described by the manufacturer. Slides were subsequently incubated with rabbit anti-tenascin-XB antibody (Proteintech, Inc; Chicago, IL), 1:50 diluted in 1% blocking solution) at 4^{o}C overnight, rinsed in PBS and Incubated with Biotinylated Anti-Rabbit IgG 1:200 (Vector Lab, BA-1000), (7.5ug/ml) diluted in 2% NGS/ PBS 60min at RT and rinsed with PBS. Sections were incubated with VECTASTAIN Elite ABC Reagent per manufacturer's guidelines for 1 hr and rinsed with PBS. Antibody staining was revealed using the DAB Peroxidase Substrate Kit (Vector lab, SK-4100) per manufacturer's guidelines. Sections were rinsed with distilled water, dehydrated through an ethanol/xylene series, cover-slipped and visualized under light microscopy. Images are captured using the image capture software in the Microscopy core at the University of Iowa. B.) For Immunofluorescence: slide sections were then rinsed with distilled water, PBS and incubated with 5% normal goat serum/5% Bovine Serum Albumin for 1 hr at room temp.

Slides were incubated with primary antibody (rabbit anti-tenascin-XB, 1:50 diluted in 1% blocking solution) at 4^{o}C overnight, rinsed with PBS and incubated with Dilute Fluorescent 2nd antibody with 1% blocking solution (Alexa Fluor® goat anti-Rabbit 568 1:200) for 1.5 - 2hr at RT, covered from the light. Slides were rinsed with PBS and underwent aqueous mounting, with removal of any remaining buffer and application of 2-3 drops of VECTASHIELD® Mounting Medium (Catalog # H-1000) and coverslipped and allowed to dry for 20 minutes in the dark. Confocal images were obtained immediately using the equipment available in the University of Iowa Microscopy core.

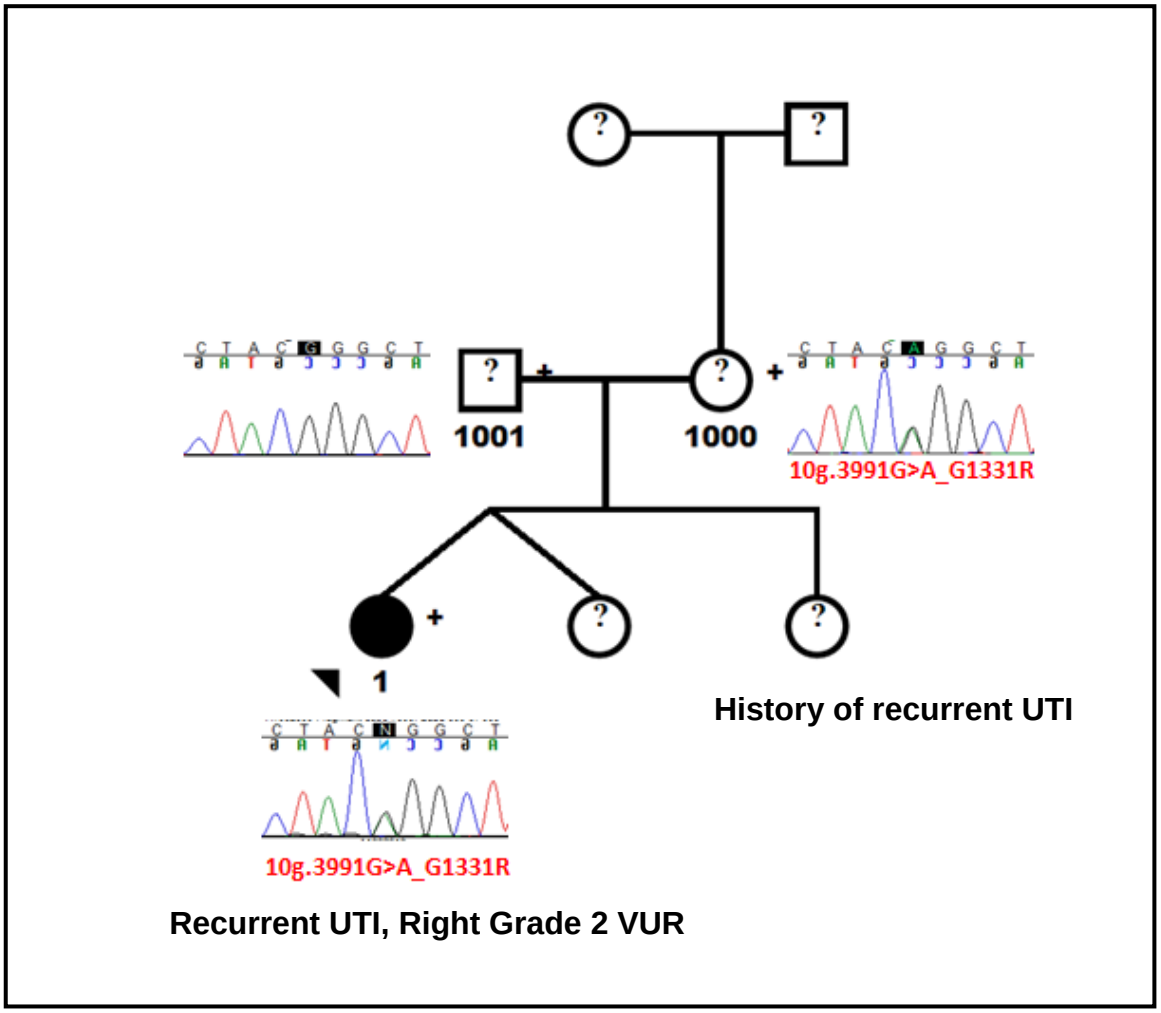

Figure S1: Pedigree of second family with G1331R mutation. Squares are males and circles are females. Filled shape denote affected individuals, shapes with question mark denote unknown phenotype. The proband (individual 1) has right grade 2 VUR, her mom (Individual 1000) never had VCUG done. The proband and her mom have the G1331R change.

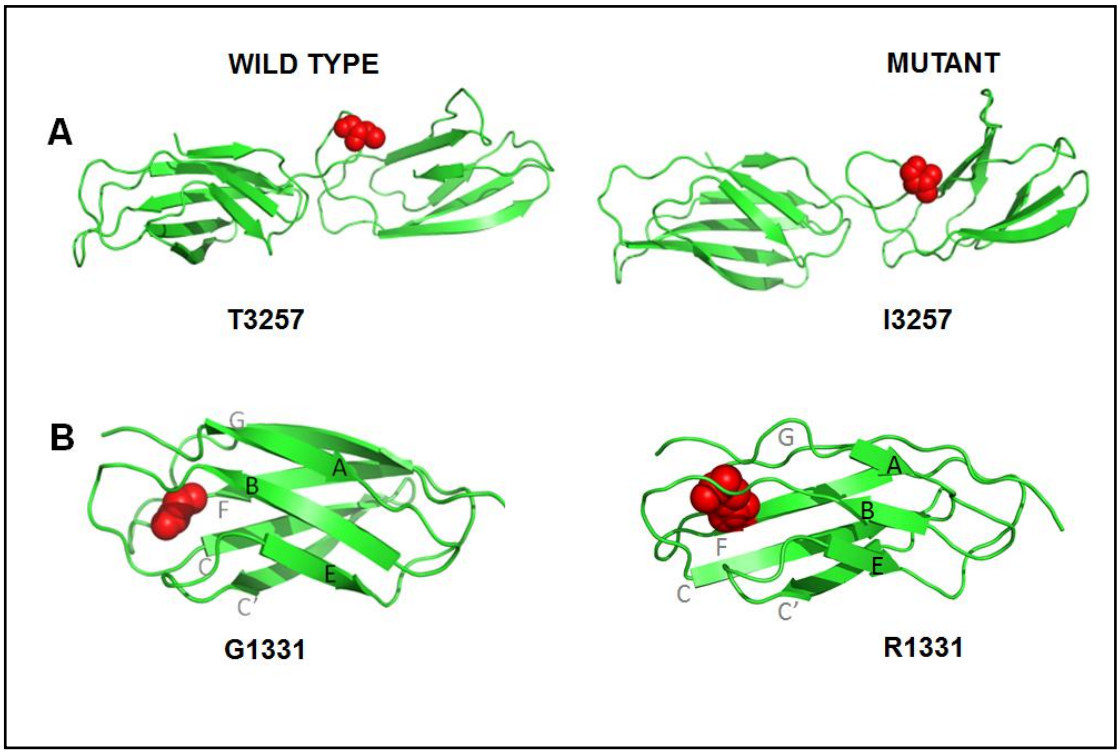

Figure S2: Location of TNXB mutations in three-dimensional models of the TNXB fibronectin Type III (FnIII) domains. (A) I-TASSER was used to model the structure of TNXB FnIII domains 23 and 24. Residue T3257 (in red) is predicted to reside in the linker between the two fibronectin domains, modeling the T3257I mutation results in some structural changes. (B) The structure of the 5th FnIII domain of human TNXB was predicted using the I-TASSER server for homology modeling. The beta strands are labeled as designated by Leahy et al. and residue G 1331 is shown as a space-filling model highlighted in red. Structural modeling of the 5th FnIII domain containing the G1331R mutation (again highlighted in red) resulted in, perturbation of the secondary structure of the protein.

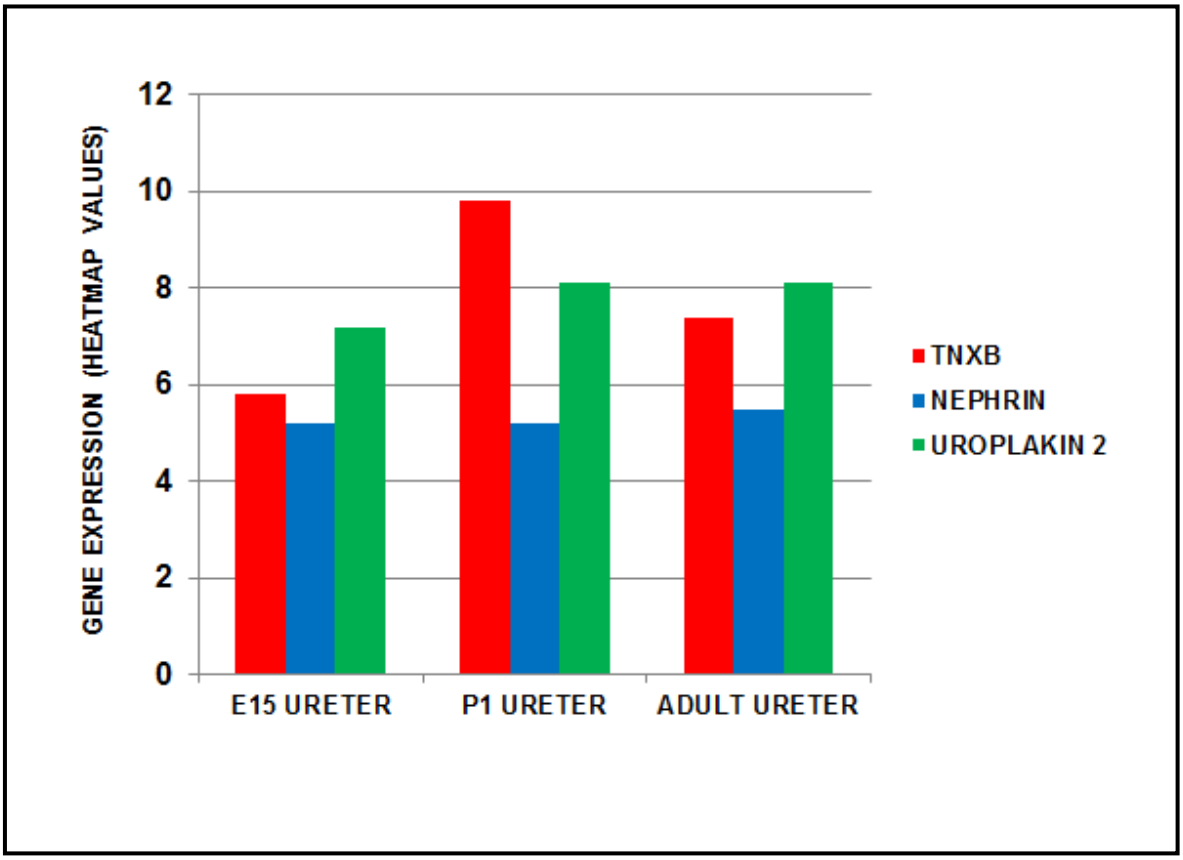

Figure S3: Microarray expression data for TNXB, nephrin and uroplakin II in mouse ureter. TNXB is expressed from E15 (Embryonic day 15) and is persistent post natally (P1: postnatal day1) and also in adult ureter, it is relatively more abundant than nephrin a key podocyte gene at every time point but similar to uroplakin II a gene that is enriched in the developing lower genitourinary tract. Relative expression of each gene in Heatmap value is derived from average of three different data set. Data is derived from the publicly available Genitourinary Molecular Anatomy Project (www.gudmap.org).

Table S1: Exclusion of previously reported loci for VUR/CAKUT in family 6606

LOCI	MLOD SCORE IN FAMILY 6606
Chromosome 1p13	-9.7
SOX11 Chrom2	-8.3
ROBO2 Chrom3	-11.0
FRAS1/SPRY1 Chrom4	-9.1/-0.54
GDNF Chrom5	-10.0
CDC5L Chrom6p21	3.3*
TOP1MT/SOX17/Chrom8q24	-8.2/-1.1/-8.3
Chrom10q26	-16.3
EMX2	-15.6
PAX2	-16.4
RET	-14.8
NAT10 Chrom11	-11.8
Chromosome12p11	-9.1
FREM2 Chrom13	-8.9
ANGEL1 Chrom14	-4.5
HNF1B Chrom17	-14.7
USF2 Chrom19	-8.5
UPK3A	-12.4

*Mutations in CDC5L was excluded in family 6606 by direct exon sequencing

Table S2: Primer sequences for TNXB

Primer Name	Primer Sequence
TNXB-2F	CCTCATGGTGAGGAAGGAGT
TNXB-2R	TCTCCTTTTTGAAGCTGCTCT
TNXB-3.1F	ATGCCACAGTCGTCACCA
TNXB-3.1R	AGAGCAGAGCTGGGCTACAT
TNXB-3.2F	GCAATCGGTTCCAGTGTACC
TNXB-3.2R	GGTCGTTGCGTGTGCTTT
TNXB-3.3F	GCAGTCTTCCCCTGAGTAGC
TNXB-3.3R	GAATGCATTTGCGACACG
TNXB-3.4F	AGGCACACTCCTTGCACAC
TNXB-3.4R	GAGAACGGCGTGTGTGTTT
TNXB-3.5F	CCCTCTACACACACACTGG
TNXB-3.5R	GGAAGGCTACGTGAGTGAGG
TNXB-3.6F	CATGCTCTCCCTCCACTCTT
TNXB-3.6R	GTGCAAGGAGTGTGCCTGT
TNXB-4F	GCCATCTGGACTCAACCAAT
TNXB-4R	CTGAGTAAAAGGGGCTGTGG
TNXB-5F	GGCAGATTCCCTCTCTAGTCC
TNXB-5R	GAGATAAGGGGGATTGAGCA
TNXB-6F	CCAGAAGCATTCAGAGGAGTC
TNXB-6R	TGGACTAGAGAGGGAATCTGC
TNXB-7F	CCAATAACCCCAGCTCCTC
TNXB-7R	GGACTGGGGATTCCTTTCTAGT
TNXB-8F	CCCAAAGCACTGAGAAAACC
TNXB-8R	ATCCAGGATGGAGTGAGGTG
TNXB-9F	CTGACACAGCCAGGGTATGA
TNXB-9R	CCTATGTGGGATTTGGCTTC
TNXB-10F	GGCAAAATGAGCTGAGAAGG
TNXB-10R	TGTCAGGCTTCCCAGAAGTT
TNXB-11F	CTGGAGCAAGGAGAGCAACT
TNXB-11R	TTTCCATGGCTGTCATCTGT
TNXB-12F	GGAGGAGTAAAGGGGTCAGG
TNXB-12R	GGTGACAGCGAGACTCCATC
TNXB-13F	CAGGTGGACAAAGGGAAGAC
TNXB-13R	CCCCATCTCAGTTCACAGC
TNXB-14F	CTGGGGCCAAATAATGGTAA
TNXB-14R	GCAGTTCTGGGTTTTTCCAG
TNXB-15F	AAAGGGGCACAAGGAAACTT
TNXB-15R	CCCAGTCTTCCAGAAACAGC
TNXB-16F	TTCTGAAGGCTTCTCCTCCTC
TNXB-16R	TTTCGATTGCTGACTGCTTG
TNXB-17F	ACCAAAGAGCAAGAGGGTGA
TNXB-17R	CTTTCAGATGGCTGGGAGAG
TNXB-18F	AGGAGATGCTGGAGGCTGTA
TNXB-18R	CCAGTCATAGCCTTGGCTTC
TNXB-19F	AGTGAAGGCACCAGCAGAA
TNXB-19R	CCTCAACACCTCCTTGCAG
TNXB-20F	ACCAAAGAGCAAGAGGGTGA
TNXB-20R	GCACCAGCATCCAGACTGT
TNXB-21F	GGTACCCATGAGGGAAAGGT
TNXB-21R	CCACGACGTAAGCACATCC
TNXB-22F	ACTGTGAGCCCCATCAAGAC
TNXB-22R	AGCAAAGCAAGTTGCCCTTA
TNXB-23F	ACCAAAGAGCAAGAGGGTGA
TNXB-23R	GGGCACTTTGTGTTTTGTGA
TNXB-24F	CATGGAAACGTGCAAAAGAA
TNXB-24R	CTTGAAGACCTGAGCACATCC
TNXB-25F	GTCAGTCCTCAGGGAAGTGG
TNXB-25R	AACAAAAGATGGCGAGGAGA
TNXB-26F	CGAAGACTGGAGAGACAGCA
TNXB-26R	CCTTCCTCACAAGACCCAAG
TNXB-27F	CCACCAGTCATCACCAAAGA
TNXB-27R	GTCCTGTTCTTGGGCACTTT
TNXB-28F	AAGAGGTGCCAAGATCCAAA
TNXB-28R	CCAGTCATAGCCTTGGCTTC
TNXB-29F	ATCAGTGGGTGCTGAGGACT
TNXB-29R	GCCGCTAAGAAATGCTCACT
TNXB-30F	GAGGGACTCACTTTCGGAGTT
TNXB-30R	ATAGCAGCCCAGGAAGCTC
TNXB-31F	TTGTCTTCAGCCCAAATGC
TNXB-31R	CTCGATCACAGCAGGGAAG
TNXB-32F	GGCAGAGCTAAAGGCCACT
TNXB-32R	GCCAAGCCTGGAAGATAAAA
TNXB-33F	CCCCGTGAAGTACAAAGACC
TNXB-33R	CAAGCTGGTGTGCTTCTGTC
TNXB-34.35F	CCCTCCTCGTTCTCTCTCAA
TNXB-34.35R	ATCTGCAGAGCGACTTCCAT
TNXB-36.37F	AGGGAAAGCAGGAAGAGGAG
TNXB-36.37R	GAGAGAACGAGGAGGGTGAA
TNXB-38.39F	ATGTCGCAAAACACGTTCAG
TNXB-38.39R	GTAGGGTCTGTGGGGTGTGT
TNXB-40.41F	ACGCGCATGGAGTAGTCAC
TNXB-40.41R	CGTGTCCACCTCTTTCACC
TNXB-42.43F	CTGTTACACTGTGGGGCTGA
TNXB-42.43R	CACAGGGACTGGGGAACTAC
TNXB-44F	AAGGACCCTGGCTCTTCTCT
TNXB-44R	CAGAGGGAGCTGGAGTTGAT

Table S3: Known and new TNXB variants in patients with VUR

RS number	Exon/Intron	Nucleotide	Amino Acid Change
rs41270461	3	607G>A	V203M
rs1150752	3	904A>G	T302A
rs204896	3	1532G>A	R511H
rs41270458	3	1734C>T	None
rs17201602	3	1949G>A	R650H
rs204900	6	2761T>G	S921A
rs185819	9	3482A>G	H1161R
rs12211410	10	3764G>A	R1255H
rs61735731	10	4010G>A	R1337H
New	14	5155G>A	V1719M
rs17207923	16	5713G>A	E1905K
rs3749962	17	6030C>T	None
rs1150756	18	6288G>A	None
rs9469081	18	6379G>A	V2127M
rs150379644	Intron 18	(+)8A>T	None
rs9469080	Intron 18	(+)11T>C	None
rs204883	19	6696C>T	None
rs2239689	Intron 20	(-)24C>T	None
rs204885	Intron 20	(+)5G>A	None
rs204886	21	7251A>G	None
rs204887	21	7440T>C	None
rs1150757	21	7461C>T	None
rs2269429	21	7483G>A	G2495S
rs1009382	22	7553G>T	G2518V
rs12196385	22	7680C>T	None
rs2066982	22	7790G>A	R2597Q
rs369637	22	7797G>A	None
rs440160	24	8192C>G	P2731R
rs17207895	26	9050A>G	K3017R
rs41258944	28	9562G>A	V3188I
rs61740331	28	9672G>A	None
rs61740337	28	9699T>C	None
rs142041833	32	10723T>C	S3575P
rs12208609	32	10782C>T	None
rs141851943	32	10893G>A	None
rs374698	33	11142G>A	None
rs2856449	33	11088T>A	None
New	33	1184G>A	None
rs397948	Intron 35	(-)45T>C	None
rs143318192	Intron 35	(-)9A>G	None
rs2894232	35	11412T>C	None
rs2395085	35	11417A>G	Q3806R
rs75024733	36	11547A>G	None
rs78089407	36	11548C>A	Q3850K
rs28361049	36	11616G>A	None
rs28361048	36	11629G>A	V3877I
rs2734313	Intron 36	(+)10G>C	None
rs1135809	38	11921A>C	N3974T
rs7742632	39	11962C>A	L3988I
rs10456399	39	12011T>C	M4004T
rs113312810	40	12156C>G	None
rs114988582	40	12170A>T	N4057I
rs4959086	40	12180C>G	C4060W
rs4959085	40	(+)5C>T	None
rs6457477	41	12224G>A	R4075H
rs4959084	43	12520G>A	D4174N
rs4959083	43	12530G>A	S4177N